

## Effects of LaPO<sub>4</sub> coating on the performance of LiNi<sub>0.5</sub>Co<sub>0.2</sub>Mn<sub>0.3</sub>O<sub>2</sub> cathode material for lithium ion batteries

Xiaodong Jiang<sup>1</sup>, Zhentao Yuan<sup>1</sup>, Jianxiong Liu<sup>1</sup>, Xin Jin<sup>2</sup>, Liying Jin<sup>3</sup>, Peng Dong<sup>1</sup>, Yingjie Zhang<sup>1</sup>, Yuhan Yao<sup>1</sup>, Qi Cheng<sup>1</sup>, Cheng Liu<sup>1</sup>, Yannan Zhang<sup>1,\*</sup>, Xiaohua Yu<sup>1,4,\*</sup>

<sup>1</sup> National and Local Joint Engineering Laboratory for Lithium-ion Batteries and Materials Preparation Technology, Key Laboratory of Advanced Battery Materials of Yunnan Province, Kunming University of Science and Technology, Kunming 650093, China.

<sup>2</sup> Shanxi Engineering Vocational College, Taiyuan 030009, China.

<sup>3</sup> Shandong Institute of Physical Education and Sports, Jinan 250102, China.

<sup>4</sup> National Engineering Research Center of Waste Resource Recovery, Kunming University of Science and Technology, Kunming 650093, China.

\*E-mail: [zyn\\_legolass@163.com](mailto:zyn_legolass@163.com), [xiaohua\\_y@163.com](mailto:xiaohua_y@163.com)

Received: 6 November 2017 / Accepted: 4 January 2018 / Published: 5 February 2018

---

LiNi<sub>0.5</sub>Co<sub>0.2</sub>Mn<sub>0.3</sub>O<sub>2</sub> (NCM-523) cathode material is coated with 2.0, 4.0 and 6.0 wt% of LaPO<sub>4</sub> via liquid phase coating method. The structure, morphology and electrochemical properties of surface modified LiNi<sub>0.5</sub>Co<sub>0.2</sub>Mn<sub>0.3</sub>O<sub>2</sub> materials are characterized by X-ray diffraction (XRD), scanning electron microscopy (SEM), electrochemical workstation, inductively coupled plasma emission spectrometry (ICP), and constant current charge and discharge test. The consequence indicates that the structure of the materials is not transformed significantly before and after coating. The cycling performance and rate capability of the coated samples are improved significantly. The capacity retention of 4 wt%-coated NCM-523 sample at 1 C and 5 C are 95.17% and 93.71% between 2.8 and 4.2 V after 100 cycles, respectively. The Correspond to capacity retention of pristine sample at 1 C and 5 C are only 77.25% and 73.16%. It can be ascribed to that LaPO<sub>4</sub> coating layer can effectively avoid the side reaction between active materials and electrolytes. Furthermore, the LaPO<sub>4</sub> coating layer can effectively reduce the dissolution of transition metal elements in electrolyte and the deposition of high impedance metal fluorides on the electrode surface.

---

**Keywords:** LiNi<sub>0.5</sub>Co<sub>0.2</sub>Mn<sub>0.2</sub>O<sub>2</sub>; cathode; coating; co-precipitation method

### 1. INTRODUCTION

As for high capacity, long service life, green environmental protection and other advantages, lithium-ion batteries (LIBs) have been widely used in portable electronic products and hybrid field. Nonetheless, the cathode material is one of the key factors that determine the properties of lithium-ion

batteries [1-4]. Compare to the currently commercial cathode materials ( $\text{LiCoO}_2$  and  $\text{LiFePO}_4$ ) [5,6],  $\text{LiNi}_{0.5}\text{Co}_{0.2}\text{Mn}_{0.3}\text{O}_2$  (NCM-523) has higher specific discharge capacity, higher voltage platform and higher energy density, as well as high conductivity, which is considered to be one of the ideal materials for the high power batteries [7-10]. While the capacity of materials decreases rapidly after long cycles under high currents, with impoverished cycle performance [11,12]. The capacity loss of materials is because of the side reaction between active materials and electrolytes, which bring about the electrode material erodes. On the one hand, the transition metal elements are dissolved in the electrolyte, on the other hand, the high resistance metal fluorides are easily deposited on the surface of electrode [13-15]. In previous reports, surface modification can reduce the side reaction between active materials and electrolytes, and effectively ameliorate the cycle life of the batteries [16-18].

The materials such as  $\text{Li}_3\text{VO}_4$  [19],  $\text{Al}_2\text{O}_3$  [20],  $\text{LiAlO}_2$  [21],  $\text{Li}_2\text{SiO}_3$  [22],  $\text{SiP}_2\text{O}_7$  [23] have been reported to be used to coat NCM-523 cathode materials to improve its electrochemical properties. Liang et al. [24] synthesized  $\text{Li}_3\text{PO}_4$  coated NCM-523 cathode materials by solid phase method, which improved the high temperature cycling performance of the material (the capacity retention of 97.4% after 50 cycles at 55 °C). Bai et al. [25] reported that  $\text{FePO}_4$  coated NCM-523 cathode materials showed significantly increased specific capacity as well as the rate capability under high cut-off voltage (the capacity retention of 91.2% after 50 cycles at 1C under a high charge cut off voltage of 4.6 V). In addition, Cho et al. [26] demonstrated that the thermal stability of  $\text{Mn}_3(\text{PO}_4)_2$  coated NCM-523 cathode materials are enhanced, compared with pristine sample (the bond energy of P=O bond is strong, and the structural stability of the material is improved). All of the results mentioned above show the cathode effects of coating on the cathode materials for lithium-ion batteries. In literature report, the strong covalent interaction between  $\text{PO}_4^{3-}$  group and metal ion can improve the thermal stability of the coating material [27]. Moreover, as a solid electrolyte,  $\text{LaPO}_4$  has good ionic conductivity and strong P=O bond, which can boost the diffusion ability of  $\text{Li}^+$  between electrode and electrolyte interface [28].

In this work, we have attempted to synthesize the different contents of  $\text{LaPO}_4$ -coated NCM-523 particles by the liquid phase coating method. Furthermore, the effects of  $\text{LaPO}_4$  coating layer amount on the structure, morphology and electrochemical properties of NCM-523 cathode materials are investigated.

## 2. EXPERIMENT

### 2.1. Preparation

Spherical  $\text{Ni}_{0.5}\text{Co}_{0.2}\text{Mn}_{0.3}(\text{OH})_2$  precursors was synthesized by co-precipitation method.  $\text{NiSO}_4 \cdot 6\text{H}_2\text{O}$ ,  $\text{CoSO}_4 \cdot 7\text{H}_2\text{O}$  and  $\text{MnSO}_4 \cdot \text{H}_2\text{O}$  were mixed in deionized water ( $n(\text{Ni}): n(\text{Co}): n(\text{Mn}) = 5: 2: 3$ ). The mixtures were heated at 70 °C in the reaction still,  $\text{NH}_3 \cdot \text{H}_2\text{O}$  (5 wt%) and NaOH (5 mol/L) were added to the solution to control the pH value at 10-11. After that, a mixture of dehydrated  $\text{Ni}_{0.5}\text{Co}_{0.2}\text{Mn}_{0.3}(\text{OH})_2$  and  $\text{Li}_2\text{CO}_3$  ( $n(\text{Li}): n(\text{Ni}_{0.5}\text{Co}_{0.2}\text{Mn}_{0.3}(\text{OH})_2) = 1.05:1$ ) was preheated at 500 °C for 6 h and then heated at 900 °C for 10 h in air.

The coated materials were prepared by the following procedure.  $\text{La}(\text{NO}_3)_3 \cdot 6\text{H}_2\text{O}$  and  $(\text{NH}_4)_2\text{HPO}_4$  were dissolved in deionized water ( $n(\text{La}(\text{NO}_3)_3 \cdot 6\text{H}_2\text{O}) : n((\text{NH}_4)_2\text{HPO}_4) = 1 : 1$ ) and NCM-523 material was added to the solution.  $\text{NH}_3 \cdot \text{H}_2\text{O}$  (5 wt%) were added to the solution to control the pH value at 10-11 and then continuous stirring for 3 h at 70 °C. Next, the obtained precipitate was filtered and dried at 80 °C for 8 h. After that, the precursor was calcined at 500 °C for 5 h in air. By adjusting the content of  $\text{LaPO}_4$ , 2 wt%, 4 wt% and 6 wt%  $\text{LaPO}_4$ -coated NCM-523 materials are synthesized, which was labeled as 2.0 NCM-523, 4.0 NCM-523 and 6.0 NCM-523, respectively. The whole synthesis process was shown in Fig. 1.

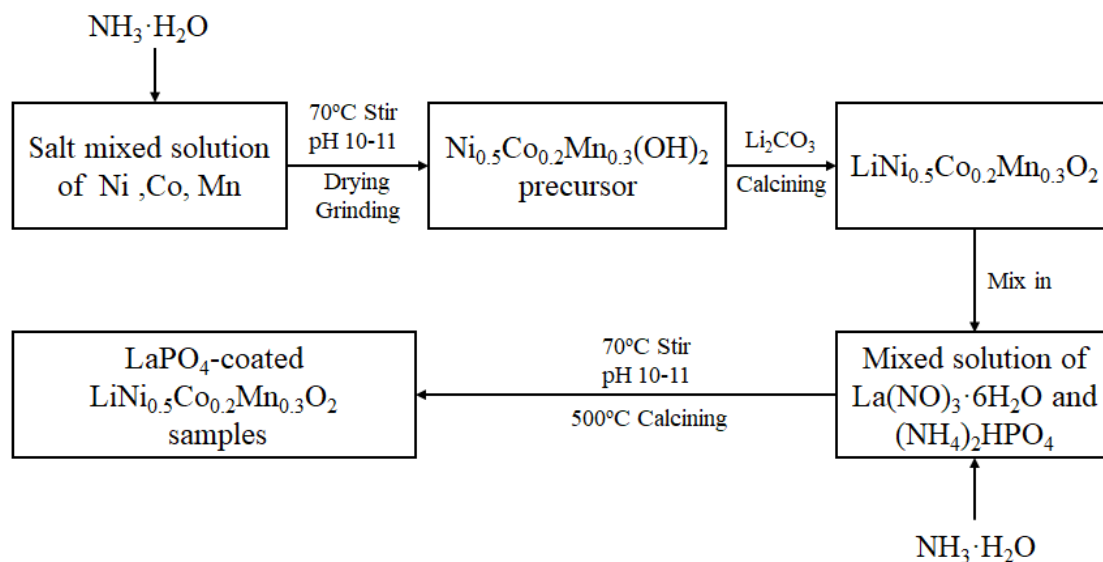


**Figure 1.** Coating process of  $\text{LiNi}_{0.5}\text{Co}_{0.2}\text{Mn}_{0.3}\text{O}_2$  with  $\text{LaPO}_4$ .

## 2.2. Characterization

The crystal structures of all the samples were characterized by X-ray diffraction (XRD, D/MAX-2200 X) equipped with  $\text{Cu K}\alpha$  radiation under test in the range of 10-80° at a scan speed of 10°  $\text{min}^{-1}$ . The surface morphology and internal structure of the pristine and  $\text{LaPO}_4$ -coated materials were observed by scanning electron microscopy method (SEM, JEOL JSM-5600LV). The elemental content of the samples before and after coating is analyzed by inductively coupled plasma atomic emission spectrometry (ICP).

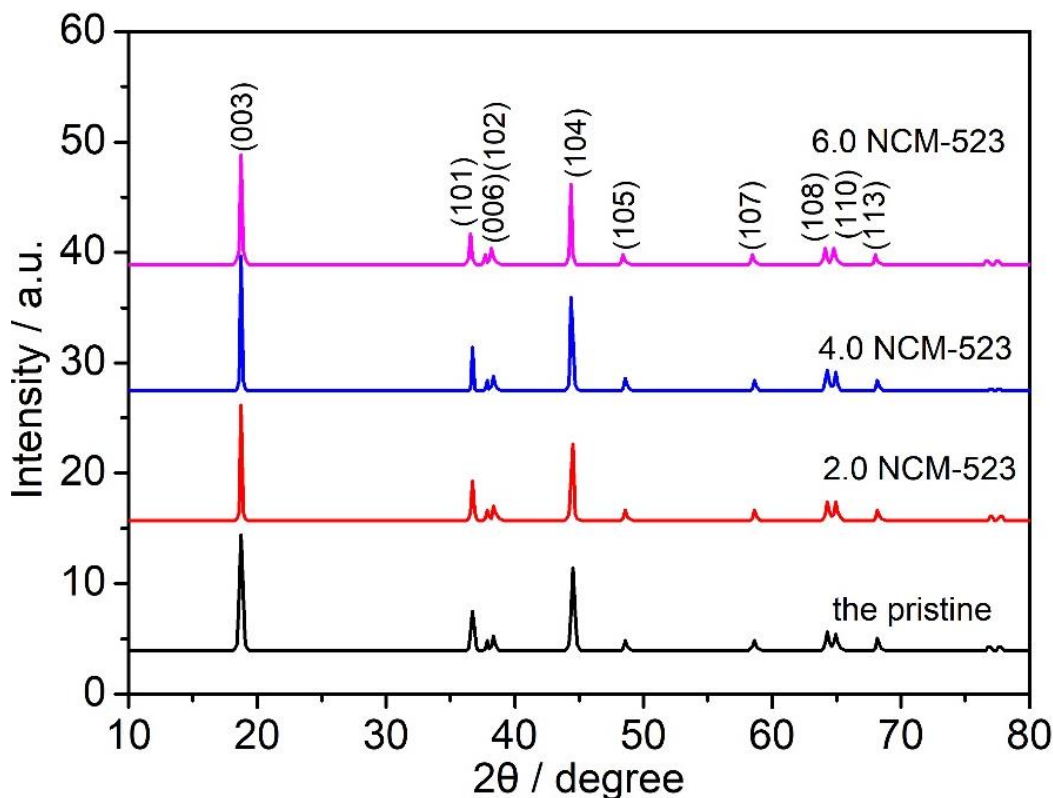
## 2.3. Electrochemical measurements

The electrochemical performances were performed using a standard CR2025 coin cell. The working electrodes were composed of active materials, carbon black and PVDF (8:1:1 in weight) on Al foil. Battery assemblies were conducted in an argon-filled glove box using lithium metal foil was used as anode, a Celgard 2400 polypropylene film as the separator and 1 M  $\text{LiPF}_6$  in ethylene carbonate (EC), dimethyl carbonate (DMC) and ethylmethyl carbonate (EMC) (1:1:1 in volume) as the electrolyte. The charge/discharge properties were tested using a CT-3008 battery test system

(Shenzhen Newware Electronics, Ltd.) between 2.8 and 4.2 V (vs. Li/Li<sup>+</sup>). Moreover, the cyclic voltammetric curve and the electrochemical impedance were measured on a CHI 720B electrochemical workstation.

### 3. RESULTS AND DISCUSSION

The XRD patterns of pristine and LaPO<sub>4</sub>-coated NCM-523 samples are presented in Fig. 2. All diffraction peaks of materials can be indexed on the basis of a layered structure of  $\alpha$ -NaFeO<sub>2</sub> (space group:  $R\bar{3}m$ ) [29]. The clear split of the (006) / (102) and (108) / (110) for all the samples indicates the formation of a well ordered layer structure. [30]. The specific lattice parameters are calculated in Table 1. It is noted that the lattice constants of LiNi<sub>0.5</sub>Co<sub>0.2</sub>Mn<sub>0.3</sub>O<sub>2</sub> are similar to the values reported previously [31], which indicates that the LaPO<sub>4</sub> coating layer has no obvious effect on the  $\alpha$ -NaFeO<sub>2</sub> structure. Usually, the intensity ratio of (003) characteristic peak and (104) characteristic peak ( $R=I_{003} / I_{104}$ ) is used to measure the degree of cation mixing in the material, and the larger of R value, the lower of mixing degree, it is also believed that the mixing degree of cations is very low when R is higher than 1.2 [32,33]. As can be seen from Table 1 that the R is higher than 1.2 for all the samples, which indicates that all the samples have a regular cation display, the 4.0 NCM-523 exhibits the lowest cation mixing degree.

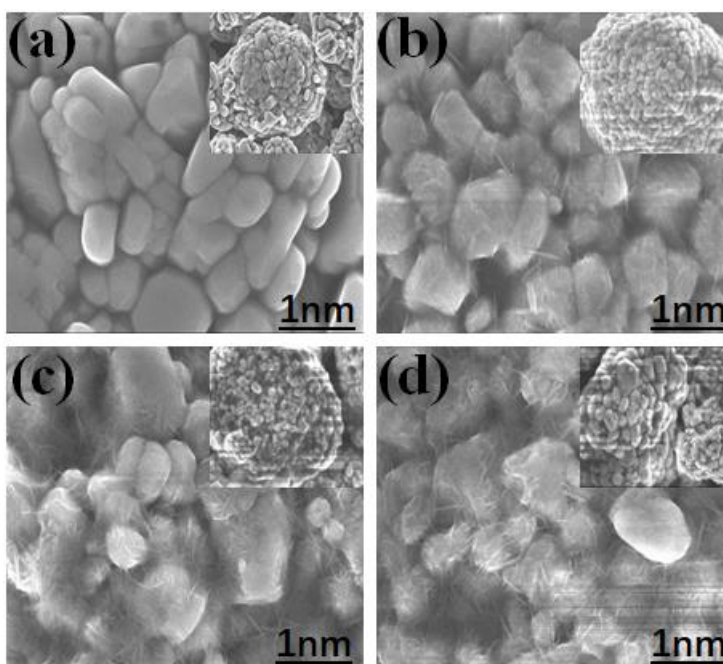


**Figure 2.** The XRD patterns of (a) pristine and LaPO<sub>4</sub>-coated samples (b) 2 wt%, (c) 4 wt%, (d) 6 wt%.

**Table 1.** Refined lattice parameters of pristine and LaPO<sub>4</sub>-coated NCM-523 samples

Sample	a / (Å)	c / (Å)	c / a	I <sub>(003)</sub> /I <sub>(104)</sub>
The pristine	2.862	14.247	4.9780	1.2434
2.0 NCM-523	2.862	14.245	4.9773	1.2482
4.0 NCM-523	2.864	14.248	4.9747	1.2593
6.0 NCM-523	2.863	14.249	4.9769	1.2517

Fig. 3 illustrates the SEM images of pristine and LaPO<sub>4</sub>-coated NCM-523 samples at low and high magnifications. Obviously, the fundamental particles of NCM-523 have irregular polyhedron structure with a particle size of about 0.5-1 μm, and the secondary particles agglomerate into class spherical with a particle size of 10-15 μm, the secondary size of samples coated with LaPO<sub>4</sub> are not changed significantly. Moreover, Fig. 3(b-d) clearly indicates that LaPO<sub>4</sub> is coated on the surface of NCM-523 particles, and the coating on NCM-523 particles becomes intensive with the increase of coating amount.

**Figure 3.** The SEM images of pristine (a), and LaPO<sub>4</sub>-coated samples (b) 2.0 wt%, (c) 4.0 wt% and (d) 6.0 wt%.

For the purpose of examining whether LaPO<sub>4</sub> nano particles are coated successfully, the composition and distribution of elements on the surface of 2.0 NCM-523 sample are examined by energy-dispersive X-ray spectrometer (EDS). The EDS mapping (Fig. 4) results show that the elements (La and P) are homogeneous distribution on the surface of 2.0 NCM-523 sample, indicating that the LaPO<sub>4</sub> particles are successful coated on the surface of NCM-523 samples.

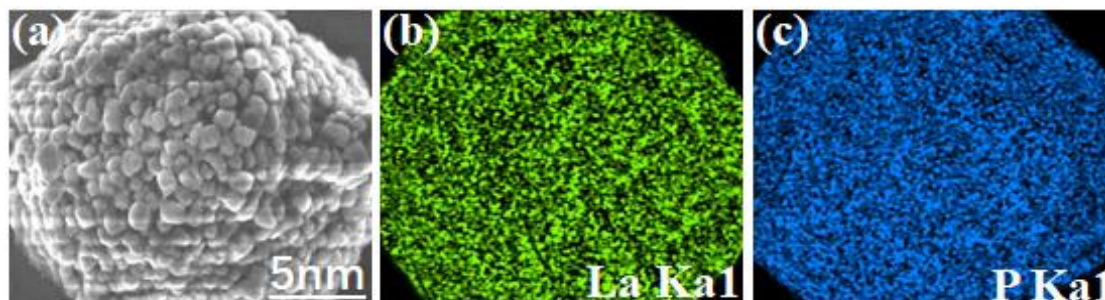


**Figure 4.** The EDS mappings of 2.0 NCM-523 sample.

In order to examine the electrochemical properties of the coated material, the electrochemical tests are conducted. Fig. 5 exhibits the initial charge/discharge curves of pristine and  $\text{LaPO}_4$ -coated NCM-523 samples between 2.8 and 4.2 V at 1 C ( $1 \text{ C} = 180 \text{ mAh g}^{-1}$ ). In the course of charging, for all the samples, there is a voltage plateau around 3.65 V. After that, the curves linearly increase to 4.2 V, which corresponds to the oxidation reaction of  $\text{Ni}^{2+} \rightarrow \text{Ni}^{4+}$ . In the course of discharging, for all the samples, there is a voltage plateau around 3.55 V when the voltage drops rapidly. After that, the curves linearly decrease to 4.2 V, which corresponds to the oxidation reaction of  $\text{Ni}^{2+} \rightarrow \text{Ni}^{4+}$  [34,35]. The relevant charge/discharge data are shown in Table 2. It noted that the first charge and discharge capacities of pristine NCM-523 are 172.2 and 155.1  $\text{mAh g}^{-1}$ , respectively. The initial coulombic efficiency is 90.07%. However, the initial coulombic efficiencies of 2.0 NCM-523, 4.0 NCM-523 and 6.0 NCM-523 are 92.89%, 94.21% and 92.34%, respectively. Which indicates that  $\text{LaPO}_4$  coating layer can improve the initial coulombic efficiency of NCM-523 samples. The discharge capacity of  $\text{LaPO}_4$ -coated samples is slightly lower than that of the pristine sample because the ratio of the active material is decreased upon surface coating [36].

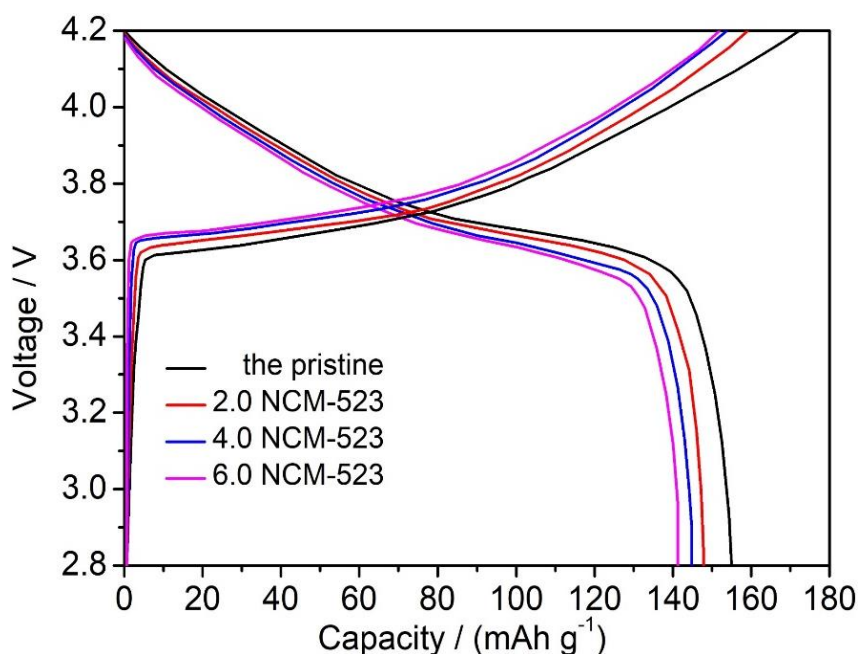


**Figure 5.** The initial charge and discharge curves of the pristine and  $\text{LaPO}_4$ -coated NCM-523 samples between 2.8 and 4.2 V at 1 C.

**Table 2.** The initial charge and discharge data of pristine and LaPO<sub>4</sub>-coated NCM-523 samples at 1 C

Sample	Initial charge capacity (mAh g <sup>-1</sup> )	Initial discharge capacity (mAh g <sup>-1</sup> )	Initial coulombic efficiency (%)
The pristine	172.2	155.1	90.07%
2.0 NCM-523	159.1	147.8	92.89%
4.0 NCM-523	153.7	144.8	94.21%
6.0 NCM-523	152.9	141.2	92.34%

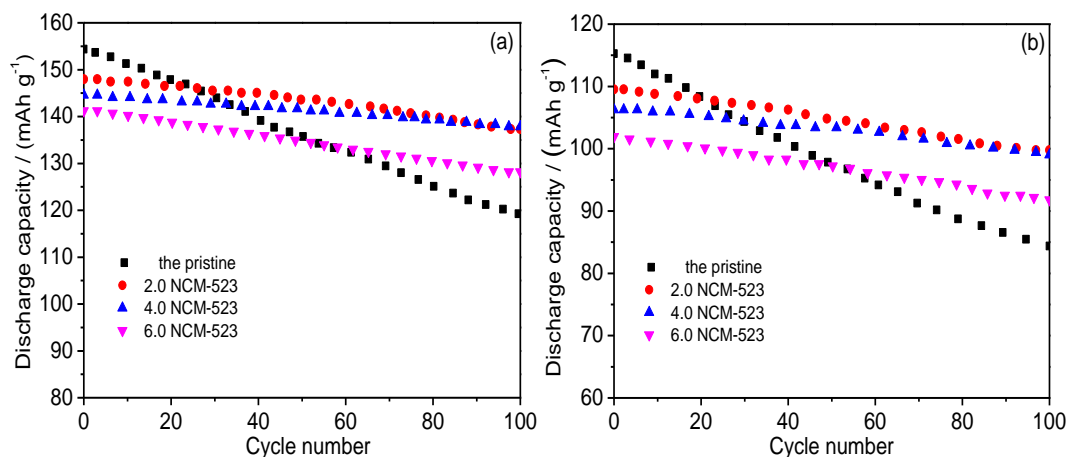
**Figure 6.** The cycling performance of pristine and LaPO<sub>4</sub>-coated samples between 2.8 and 4.2 V at (a) 1 C and (b) 5 C.

Fig. 6 (a) and 6 (b) shows the cycling performance of pristine and LaPO<sub>4</sub>-coated NCM-523 samples between 2.8 and 4.2 V at 1 C and 5 C, respectively. The relevant cycling performance data are shown in Table 3. The result indicates that all the coated samples exhibit higher discharge capacities and capacity retention than the pristine one, and the 4.0 NCM-523 sample exhibits the favorable cycling performance. The discharge capacity of the pristine sample decreases sharply from 154.3 to 119.2 mAh g<sup>-1</sup> at 1C after 100 cycles, only 77.35% discharge capacity left. Furthermore, the capacity retention of the pristine sample is only 73.16% at 5 C after 100 cycles. For the 4.0 NCM-523 sample, the capacity retention of 95.17% and 93.71% at 1 C and 5 C after 100 cycles, respectively. The excellent capacity retention of 4.0 NCM-523 sample may be attributed to the surface modification of LaPO<sub>4</sub>. The LaPO<sub>4</sub>-coated NCM-523 samples can effectively inhibit the side reactions between active materials and electrolyte caused by HF etching. [37,38].

We compared the cycle performance of LaPO<sub>4</sub>-coated NCM-523 cathode materials with other similar compound-coated NCM-523 cathode materials. The relevant comparison data is shown in the Table 4. It is noted that the LaPO<sub>4</sub>-coated NCM-523 cathode material exhibits good capacity retention (95.17%) compared to other similar compound-coated NCM-523 cathode materials. It is proved that the coating modification of LaPO<sub>4</sub> is an effective method to improve the cycling performance of NCM-523 cathode material.

**Table 3.** The cycling performance data of pristine and LaPO<sub>4</sub>-coated NCM-523 samples at 1 C and 5 C

Sample	The pristine	2.0 NCM-523	4.0 NCM-523	6.0 NCM-523
1 C-Initial discharge capacity (mAh g <sup>-1</sup> )	154.3	147.8	144.8	141.2
1 C-100th discharge capacity (mAh g <sup>-1</sup> )	119.2	137.3	137.8	129.8
1 C-capacity retention after 100 cycles (%)	77.25%	92.89 %	95.17%	92.05%
5 C-initial discharge Capacity (mAh g <sup>-1</sup> )	115.3	109.5	106.2	101.9
5 C-100th discharge Capacity (mAh g <sup>-1</sup> )	84.36	100.2	99.52	92.80
5 C-capacity retention after 100 cycles (%)	73.16%	91.51 %	93.71%	91.06%

The rate capacities of pristine and LaPO<sub>4</sub>-coated NCM-523 samples between 2.8 and 4.2 V are shown in Fig. 7. It is noted in Fig. 7 that the capacity of pristine NCM-523 sample decreases rapidly with the cycles and the increase of current density, while the LaPO<sub>4</sub>-coated NCM-523 samples obviously exhibits better rate capability than uncoated one at the higher current rates. The relevant rate capacities data are shown in Table 5. Noticeably, the discharge capacities of pristine NCM-523 sample are 170.8 mAh g<sup>-1</sup>, 160.1 mAh g<sup>-1</sup>, 149.5 mAh g<sup>-1</sup>, 135.2 mAh g<sup>-1</sup>, 119.1 mAh g<sup>-1</sup> and 89.6 mAh g<sup>-1</sup> at 0.1 C, 0.2 C, 0.5 C, 1 C, 2 C and 5 C, respectively.

**Table 4.** The comparison with the cycling performance of similar cathode materials

Coating materials of NCM-523	Capacity retention and discharge capacity (mAh g <sup>-1</sup> ) after several cycles at certain rate
LaPO <sub>4</sub> (our work)	95.17%, 137.8 mAh g <sup>-1</sup> , 100 cycles, 1 C
Li <sub>3</sub> VO <sub>4</sub> [19]	83.54%, 137.1 mAh g <sup>-1</sup> , 100 cycles, 1 C
LiAlO <sub>2</sub> [21]	91%, 202 mAh g <sup>-1</sup> , 100 cycles, 1 C
Li <sub>2</sub> SiO <sub>3</sub> [22]	83%, 149.82 mAh g <sup>-1</sup> , 100 cycles, 0.2 C
SiP <sub>2</sub> O <sub>7</sub> [23]	91%, 165 mAh g <sup>-1</sup> , 40 cycles, 0.5 C
FePO <sub>4</sub> [25]	91.2%, 185.9 mAh g <sup>-1</sup> , 50 cycles, 1 C
Mn <sub>3</sub> (PO <sub>4</sub> ) <sub>2</sub> [26]	92.6%, 153 mAh g <sup>-1</sup> , 50 cycles, 0.5 C



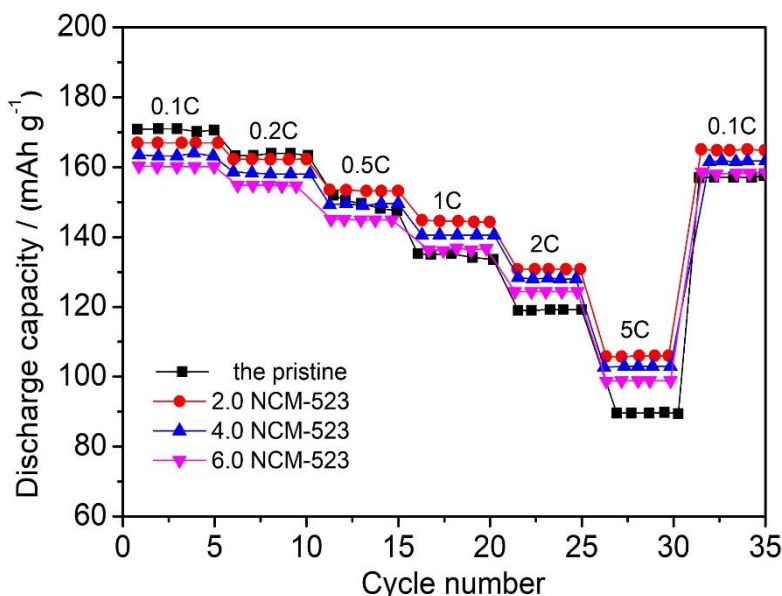


**Figure 7.** The rate performance of the pristine and LaPO<sub>4</sub>-coated NCM-523 samples.

Furthermore, the capacity retention relative to 0.1 C is 93.76%, 87.49%, 79.17%, 69.66% and 52.42% at 0.2 C, 0.5 C, 1 C, 2 C and 5 C, respectively. However, the discharge capacities of 4.0 NCM-523 sample are 163.5 mAh g<sup>-1</sup>, 158.6 mAh g<sup>-1</sup>, 149.3 mAh g<sup>-1</sup>, 140.6 mAh g<sup>-1</sup>, 128.5 mAh g<sup>-1</sup> and 102.7 mAh g<sup>-1</sup> at 0.1 C, 0.2 C, 0.5 C, 1 C, 2 C and 5 C, respectively, and the capacity retention relative to 0.1 C is 96.95%, 91.28%, 85.96%, 78.54% and 62.80% at 0.2 C, 0.5 C, 1 C, 2 C and 5 C, respectively. Compared with pristine NCM-523 sample, the capacity retention of LaPO<sub>4</sub>-coated NCM-523 samples is obviously increased, which indicates that the surface coating modification of LaPO<sub>4</sub> can improve the rate capacities of NCM-523 samples. The improvement of rate capacity may be attributed to the fact that LaPO<sub>4</sub> coating layer display good ionic conductivity, which enhances the diffusion capacity of Li<sup>+</sup> between the electrode and the electrolyte interface, and finally improve the electrochemical reversibility of active materials [39].

**Table 5.** The rate performance data of the pristine and 4.0 NCM-523 samples at different rates

Sample		0.1 C	0.2 C	0.5 C	1 C	2 C	5 C
The pristine	Discharge capacity /(mAh g <sup>-1</sup> )	170.8	160.1	149.5	135.2	119.1	89.6
	Capacity retention (Relative to 0.1 C)		93.76%	87.49%	79.17%	69.66%	52.42%
4.0 NCM-523	Discharge capacity /(mAh g <sup>-1</sup> )	163.6	158.6	149.3	140.6	128.5	102.7
	Capacity retention (Relative to 0.1 C)		96.95%	91.28%	85.96%	78.54%	62.80%

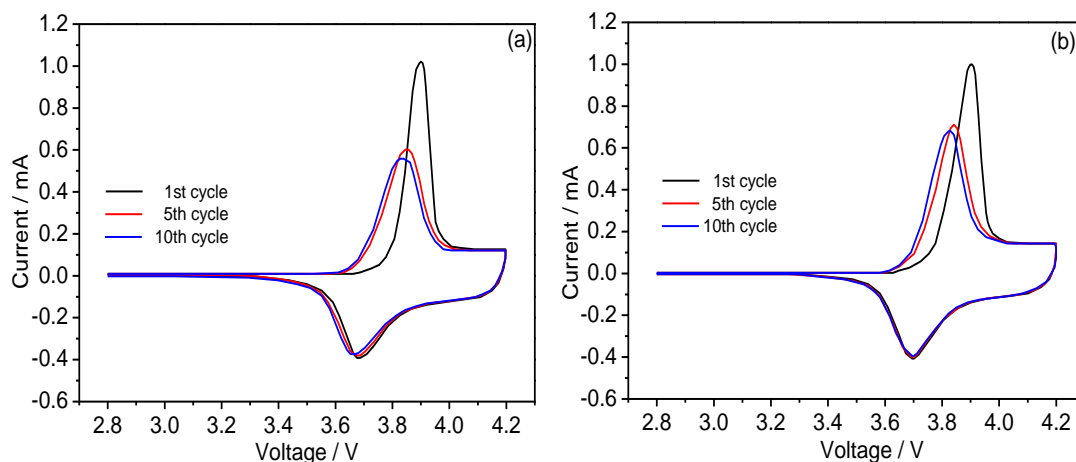


**Figure 8.** Cyclic voltammograms (CV) of (a) pristine and (b) 4.0 NCM-523 samples between 2.8 and 4.2 V.

The cyclic voltammograms (CV) of pristine and 4.0 NCM-523 samples between 2.8 and 4.2V after 1st, 5th, 10th cycles at a scan rate of 0.1mV/s are shown in Fig. 8(a) and 8(b), respectively. Obviously, all the samples have a pair of apparent redox peaks in the range of 2.8-4.2 V, which corresponding to the redox reaction of  $\text{Ni}^{2+} / \text{Ni}^{4+}$ . The electrochemical reversibility of the electrode is generally reflected by the redox reaction gap (V) between the anodic peak and cathodic peak [40]. For the pristine sample, the Lithium stripping oxidation potential of  $\text{Ni}^{2+} \rightarrow \text{Ni}^{4+}$  sample are 3.906 V, 3.857 V and 3.839 V after 1st, 50th, 100th cycles, respectively. Furthermore, the lithium intercalation reduction potential of  $\text{Ni}^{4+} \rightarrow \text{Ni}^{2+}$  are 3.686 V, 3.675 V and 3.652 V, respectively. The redox reaction gaps ( $\Delta V$ ) of 4.0 NCM-523 samples are 0.188, 0.14 and 0.128, respectively, which are reduced than the uncoated one. The result indicates that the polarization of active materials after  $\text{LaPO}_4$  coating layer is inhibited and the reversible property is enhanced effectively.

To further examination the electrochemical properties of  $\text{LaPO}_4$ -coated NCM-523 cathode material. The electrochemical impedance spectroscopy (EIS) spectra of pristine and  $\text{LaPO}_4$ -coated samples have been measured between 2.8 and 4.8 V (after 1 cycle, 50 cycles and 100 cycles), as shown in Fig. 9. It is noted that all EIS curves are made up of the semi-circle of the high to medium frequency region and the oblique line of the low frequency region. The semi-circle of the high to medium frequency region represents the charge transfer resistance ( $R_{ct}$ ), and the oblique line of the low frequency region corresponds to the Warburg impedance ( $W_o$ ) [41,42]. The EIS maps are simulated by the equivalent circuit (Fig. 9c) and the fitting values data of  $R_{ct}$  and  $R_s$  are listed in Table 6. The  $R_{ct}$  value of the pristine sample increased from 55.47 V to 481.7 V after 100 cycles. However, the  $R_{ct}$  value of the 4.0 NCM-523 also increased from 52.17 V to 157.3 V after the same cycles. Evidently, the  $R_{ct}$  value of the pristine sample is remarkably larger than that of the  $\text{LaPO}_4$ -coated samples. It can be ascribed to that the  $\text{LaPO}_4$  as a solid electrolyte can form a solid electrolyte interface to prevent the electrolyte from corroding the active material, and promote the diffusion of  $\text{Li}^+$  and electrons at the electrolyte and electrode interface. This analysis implies that  $\text{LaPO}_4$  coating layer can effectively inhibit the side reactions between active materials and electrolyte. Furthermore, the  $\text{LaPO}_4$  coating

layer can promote the efficiency of electronic transmission. Which corresponds to the previous test results of cycling and rate performance.

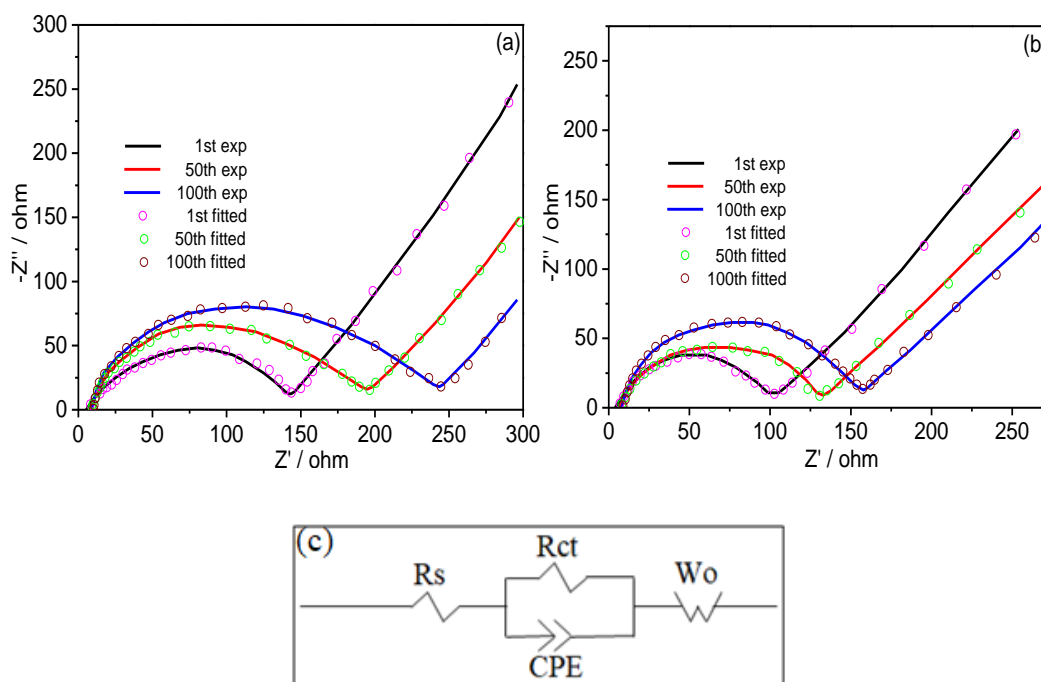


**Figure 9.** Nyquist curves of (a) pristine and (b) 4.0 NCM-523 after 1st, 50th, 100th.

**Table 6.** Impedance data of pristine and 4.0 NCM-523 after different number of cycles at equilibrium state

Cycle number	The pristine		4.0 NCM-523	
	Rs/ohm	Rct/ohm	Rs/ohm	Rct/ohm
1st	6.620	55.47	4.322	52.17
50th	8.871	205.9	6.916	100.4
100th	10.49	481.7	8.645	157.3

All the samples are stored in electrolyte for 15 days, and the content of LaPO<sub>4</sub> in coated samples and the dissolved amount of transition metal in electrolyte is measured by inductively coupled plasma emission spectrometer (ICP). The ICP test data are shown in Table 7. It is noted that the contents of LaPO<sub>4</sub> in 2.0 NCM-523, 4.0 NCM-523 and 6.0 NCM-523 samples are 1.726%, 3.612% and 5.371%, respectively, and the errors are less than 15% compared with theoretical values. In addition, the dissolving amount of transition metal ions of LaPO<sub>4</sub>-coated samples in electrolyte is significantly reduced storage 15 days compared with the pristine sample. It proves that the LaPO<sub>4</sub> coating layer can effectively inhibit the transition metal dissolution of the cathode materials in the electrolyte, thus improving the cycling and rate performance of the active material.

**Table 7.** The ICP test data of the pristine and LaPO<sub>4</sub>-coated samples

Sample	The content of LaPO <sub>4</sub>	The error of theoretical content of LaPO <sub>4</sub>	Dissolved amount of Mn <sup>2+</sup> in electrolyte (after storage 15 days ) / ppm	Dissolved amount of Co <sup>2+</sup> in electrolyte (after storage 15 days ) / ppm	Dissolved amount of Ni <sup>2+</sup> in electrolyte (after storage 15 days ) / ppm
The pristine	—	—	247.2	176.4	384.9
2.0 NCM-523	1.726%	13.7%	88.93	65.72	136.5
4.0 NCM-523	3.612%	9.7%	55.74	38.16	88.23
6.0 NCM-523	5.371%	10.5%	52.33	36.74	82.51

#### 4. CONCLUSIONS

In this work, LaPO<sub>4</sub>-coated NCM-523 cathode materials with different content (2 wt%, 4 wt%, 6wt%) are successfully prepared by liquid phase coating method. The cycling and rate performances of LaPO<sub>4</sub>-coated samples are improved significantly. The 4.0 NCM-523 sample has the favorable cycling and rate performance. The capacity retention at 1 C and 5 C are 95.17% and 93.71% after 100 cycles, respectively. While the capacity retention of pristine NCM-523 sample at 1 C and 5 C are only 77.25% and 73.16%, respectively. Furthermore, the LaPO<sub>4</sub> coating layer can effectively reduce Rct of the cathode materials. The performance improvement of LaPO<sub>4</sub>-coated samples indicates that LaPO<sub>4</sub> has good ion conductivity which can improve the diffusion capacity of Li<sup>+</sup> between electrode and electrolyte interface. The modification of LaPO<sub>4</sub> is proved to be an effective measure to improve the cycling and rate performance of the cathode material for LIBs. This effective strategy can be applied to other cathode materials of LIBs for better cycle life.

#### ACKNOWLEDGEMENTS

This work was supported financially by the National Nature Science & Foundation of China (grant Nos. 51665022 and 51601081).

#### References

1. R. Ju, M. Kun, Y.X. Hua, Z.Y. Nan, *Int. J. Electrochem. Sci.*, 12 (2017) 11987.
2. L. Cheng, R. Ju, Z.Y. Nan, Y.X. Hua, L.J. Xiong, Z.Z. Lin, *Int. J. Electrochem. Sci.*, 12 (2017) 9914.
3. C. Qi, L. Cheng, M. Kun, Y.X. Hua, Z.Y. Nan, L.J. Xiong, J. Xin, J.L. Ying, *Int. J. Electrochem. Sci.*, 13 (2018) 265.

4. W. Xiao, Z.Y. Nan, L. Cheng, Y.Z. Tao, Y.X. Hua, Z. Yi, Z.Z. Lin, *Int. J. Electrochem. Sci.*, 12 (2017) 12009.
5. Z.Y. Nan, D. Peng, Z.M. Yu, S.X. Liang, Y.X. Hua, S.J. Jie, M. Qi, Li. Xue, Z.Y. Jie, *J. Appl. Electrochem.*, doi:10.1007/s10800-017-1136-4.
6. D. Belov, Y.M. Hua, *J. Solid State Electrochem.*, 12 (2008) 885.
7. W. Jiang, L.J. Xiong, D.Y. Chun, Z. Yi, *Adv. Mater. Res.*, 9 (2013) 301.
8. S.-M. Bak, H.E. Yuan, Z.Y. Ning, Y.X. Qian, S.D. Senanayake, S.-J. Cho, K.-B. Kim, K.Y. Chung, Y.X. Qing, K. Wan, *Acs Appl. Mat. Interfaces*, 6 (2014) 2259.
9. S.K. Jung, H. Gwon, J. Hong, K.-Y. Park, D.-H. Seo, H. Kim, J. Hyun, W. Yang, K. Kang, *Adv. Eng. Mater.*, 4 (2014) 94.
10. Y.H. Jun, Q.Y. Ming, T.D. Ming, G.S. Hua, Z.Y. Bei, Z.H. Shen, *Energy Environ. Sci.*, 7 (2014) 1068.
11. S. Hong, Z.K. Jie, *J. Phys. Chem. C*, 121 (2017) 6002.
12. L. Xia, Q.K. Hui, G.Y. Yan, Z.F. Dong, *J. Mater. Sci.*, 50 (2015) 2914.
13. C.S. Hai, W. Yi, L.T. Chao, D.W. Jun, H.Z. Xiang, S.Y. Tao, L. Hao, L.M. Fan, G. Hua, D.Y. Dong, W.W. Dong, R.M. Min, Z.J. Xin, W.X. Wei, P. Feng, *Adv. Eng. Mater.*, 6 (2016) n/a.
14. H.-H. Chang, C.-C. Chang, C.-Y. Su, H.-C. Wu, M.-H. Yang, N.-L. Wu, *J. Power Sources*, 185 (2008) 466.
15. G.H. Jun, L.R. Fu, L.X. Hai, Z.X. Ming, W.Z. Xing, P.W. Jie, W. Zhao, *Trans. Nonferrous Met. Soc. China*, 17 (2007) 1307.
16. Z.L. Hua, Z. Yun, W. Fu, Z.B. Ling, W.Z. Yi, *Integr. Ferroelectr.*, 147 (2013) 103.
17. L.S. Juan, H. Chen, L.Y. Xi, L.D. Bing, C.M. He, Y.Z. Yong, L.H. Xing. *Solid State Ionics*, 179 (2008) 1754.
18. S. Ito, S. Fujiki, T. Yamada, Y. Aihara, Y. Park, T.Y. Kim, S.W. Baek, J.-M. Lee, S. Doo, N. Machida, *J. Power Sources*, 248 (2014) 943.
19. S. Tao, K.F. Jun, W.C. Qiang, S.X. Zhi, T. Xiang, C.S. Ming, H.H. Hong, Z. Lei, F. Yong, W.Z. Cheng, C.W. Sheng, Q. Bin, L. Song, *J. Alloys Compd.*, 705 (2017) 413.
20. Z. Bao, D.P. Yuan, T. Hui, Y.Y. Ying, Z.J. Chao, Y.W. Jing, Z.J. Feng, C.D. Wei, *J. Alloys Compd.*, 706 (2017) 198.
21. Z.Y. Nan, D. Peng, Y.X. Hua, X.S. Biao, S.J. Jie, Y.R. Ming, L.H. Xin, S.Z. Zhong, Y. Yao, L. Xue, Z.Y. Jie, *Int. J. Electrochem. Sci.*, 12 (2017) 6853.
22. L.L. Jun, C.Z. Yong, Z.Q. Bao, X. Ming, Z. Xiang, Z.H. Li, Z.K. Li, *J. Mater. Chem. A*, 3 (2015) 894.
23. H.G. Rong, Z.M. Fang, W.L. Li, P.Z. Dong, D. Ke, C.Y. Bing, *J. Alloys Compd.*, 690 (2017) 589.
24. Y.S. Lee, D. Ahn, Y.H. Cho, J. Cho, *J. Electrochem. Soc.*, 158 (2011) A1354.
25. S. Yang, Z.M. Hao, Q.D. Na, Y.S. Meng, *Electrochim. Acta*, 203 (2016) 154.
26. B.Y. Song, W.X. You, Y.S. Yi, Z.X. Yan, Y.X. Kang, S.H. Bo, W. Qiang, *J. Alloys Compd.*, 541 (2012) 125.
27. W. Cho, S.-M. Kim, K.-W. Lee, J.H. Song, Y.N. Jo, T. Yim, H. Kim, J.-S. Kim, Y.-J. Kim, *Electrochim. Acta*, 198 (2016) 77.
28. H.G. Song, K.-S. Park, Y.J. Park, *Solid State Ionics*, 225 (2012) 532.
29. W. Zhong, L.H. Quan, Y.Y. Ping, S.X. Yi, B.X. Tao, S.X. Ling, Z.W. Dong, L.S. Gang, *Rare Met.*, 36 (2017) 889.
30. G. Rui, S.P. Fei, C.X. Qun, D.C. Yu, *J. Alloys Compd.*, 473 (2009) 53.
31. G.Z. Liang, L.H. San, G.X. Jian, Z.Z. Ru, Y. Yong, *J. Power Sources*, 136 (2004) 139.
32. W. Feng, T. Jun, S.Y. Feng, G.Y. Biao, J. Yi, W. Zhao, H. Tao, B.L. Ying, C. Shi, *J. Power Sources*, 269 (2014) 747.
33. K.S. Fei, Q.H. Fei, F. Yao, L. Xi, W.Y. Gang, *Electrochim. Acta*, 144 (2014) 22.
34. Y. Kai, L.Z. Fan, G. Jia, Q.X. Hui, *Electrochim. Acta*, 63 (2012) 363.
35. X. Jie, N.A. Chernova, M.S. Whittingham, *Chem. Mater.*, 22 (2010) 1180.

36. P. Yue, W.Z. Xing, P.W. Jie, L.L. Jun, W. Chen, G.H. Jun, L.X. Hai, *Powder Technol.*, 214 (2011) 279.
37. L.J. Gang, W. Li, Z. Qian, H.X. Ming, *J. Power Sources*, 190 (2009) 149.
38. C.Y. Ping, Z. Yun, W. Fu, W.Z. Yi, Z. Qiang, *J. Alloys Compd.*, 611 (2014) 135.
39. J. Cho, H. Kim, B. Park, *J. Electrochem. Soc.*, 151 (2004) A1707.
40. Z.R. Rui, L.J. Xing, H.J. Jun, Z.R. Yu, Z.J. Feng, C.H. Yu, S. Guang, *J. Alloys Compd.*, 724 (2017) 1109.
41. Y.Z. Guang, G.X. Dong, W. Xiang, H.W. Bo, Z. Jun, H.F. Rong, W. Kai, X. Yao, Z.B. He, *J. Alloys Compd.*, 699 (2017) 358.
42. G.B. Appetecchi, F. Croce, L. Persi, F. Ronci, B. Scrosati, *Electrochim. Acta*, 45 (2000) 1481.
43. L.W. Bin, Z.B. Lin, *Appl. Surf. Sci.*, 404 (2017) 310.

© 2018 The Authors. Published by ESG ([www.electrochemsci.org](http://www.electrochemsci.org)). This article is an open access article distributed under the terms and conditions of the Creative Commons Attribution license (<http://creativecommons.org/licenses/by/4.0/>).